



Seismic Design of Tall Reinforced Masonry Shear Walls

Yu-Cheng Hsu^{1, *}, T.Y. Yang², and Svetlana Brzev³

¹PhD Student, Department of Civil Engineering, The University of British Columbia, Vancouver, BC, Canada

²Professor, Department of Civil Engineering, The University of British Columbia, Vancouver, BC, Canada

³Adjunct Professor, Department of Civil Engineering, The University of British Columbia, Vancouver, BC, Canada

*yhsu11@mail.ubc.ca (Corresponding Author)

ABSTRACT

The use of reinforced masonry (RM) for constructing low to mid-rise buildings in Canada has been common for over 50 years. The National Building Code of Canada 2020 (NBCC 2020) limits the height of buildings with Moderately Ductile and Ductile RM Shear Wall classes to 60 m in areas with moderate seismic activity and 40 m in areas with high seismic activity. Application of RM construction in tall reinforced masonry (TRM) buildings is extremely limited, and is likely due to limited research evidence on the seismic response of these structures. Previous research studies have examined the seismic behaviour of flexure-dominant ductile RM shear walls with different design and detailing parameters, but were mostly focused on the fully grouted RM walls constructed with commonly used blocks (200 mm thickness). Confined boundary elements have been used to enhance seismic performance and ductility of reinforced concrete (RC) shear walls for several decades. Unfortunately, there is a limited research evidence on seismic behaviour of RM shear walls with boundary elements, and there are no field applications of RM shear walls with boundary elements in Canada. This paper reviews past research studies on seismic behaviour of TRM walls, and the related research gaps. To address a gap related to seismic behaviour of TRM shear walls, a state-of-the-art hybrid simulation testing of full-scale TRM wall specimens will be performed at the University of British Columbia, and will be described in the paper. As the first phase of the research program, an experimental study on the behaviour of RM prisms simulating boundary elements in RM shear walls, has been performed by the authors. Preliminary experimental results have shown that compression capacity of the prisms predicted by the Canadian masonry design code CSA S304.

Keywords: reinforced masonry, tall reinforced masonry building, shear wall, hybrid simulation, seismic response, flexure-dominant behaviour.

INTRODUCTION

The use of reinforced masonry (RM) for construction low to mid-rise buildings in Canada has been common for over 50 years, however only a few tall reinforced masonry (TRM) buildings have been constructed at sites with low to moderate seismic hazard in central and eastern Canada [1], and outside Canada [2, 3, 4]. The application of RM construction in high-rise buildings in medium-to-high seismic hazard areas is limited, which can be attributed to limited compressive strength of commercially available concrete blocks and a lack of research studies related to seismic behaviour of TRM shear walls [5]. National Building Code of Canada 2020 (NBC 2020) [6] permits the use of Moderately Ductile and Ductile Shear Wall classes for RM buildings, but the height limit was set depending on the Seismic Category (SC), which is 60 m for SC3, and 40 m for SC4. SC3 and SC4 are categorized based on the seismic hazard index, $I_E S(0.2)$ and $I_E S(1.0)$. I_E is the importance factor and is defined as 1.0 for normal importance category under the ultimate limit state, where S denotes spectral acceleration for uniform hazard spectra at different periods (0.2 sec, 1.0 sec). SC4 category, corresponding to highest seismic zone, per NBCC 2020, refers to the seismic hazard index $I_E S(0.2)$ greater than 0.75 or $I_E S(1.0)$ greater than 0.3.

Ductile detailing provisions for reinforced masonry shear walls (RMSWs) contained in the Canadian masonry design standard CSA S304-14 [7]. Provisions related to Moderately Ductile Shear Wall (MDSW) class with ductility force modification factor R_d of 2.0 were revised, and a new class Ductile Shear Walls (DSW) with the R_d of 3.0 was introduced. MDSW class is most common for seismic design applications in Canada, and is mandatory for all post-disaster buildings according to the NBCC 2020 and CSA S304-14. Although the DSW class in NBCC 2020 and CSA 304-14 does not require

the provision of boundary elements into the walls, the importance of confinement within the end zones of the shear walls has been extensively studied as related to reinforced concrete (RC) shear walls [8, 9, 10], and the confined concrete cores are expected to provide better enhanced capacity resisting tensile and compressive stresses due to the overturning moments by delaying the (1) concrete spalling and (2) buckling of longitudinal reinforcement. Previous studies also show the importance of the 135 degree hooks and configuration of the ties in the boundary zones of the wall, which is included in the provisions for the detailing of special boundary elements in special RC shear walls in ACI 318-19 [11] and detailing of ductile RC shear walls in CSA A23.3-14 [12]. Although the concept and benefits including of providing the confined boundary elements in RC shear walls were examined, the corresponding experimental research on the RMSWs is still limited. Due to the modular nature of RM construction, the concrete blocks eliminate the possibility of continuous confined grout cores in the boundary zones of the RMSWs. In previous research studies [13, 14, 15], various boundary elements were designed and tested barbell-shaped end-confined RMSWs enclosed by three-cell flanges, two-block square boundary elements, pilaster units with spiral ties, and C-shaped block square boundary elements. Design of boundary elements was developed involved the use of new boundary blocks that were larger than regular blocks; this was required due to rare use of blocks more than 200 mm thick with limited space within hollow cores.

This paper presents an ongoing experimental project at the University of British Columbia (UBC). The project is separated into three phases: material-level prism testing, component-level wall testing and system-level hybrid simulation testing. Ductile RMSWs with embedded boundary elements using the pre-cut 250 mm hollow concrete blocks are developed for the application of TRM buildings. The paper also reports the preliminary findings from material testing of unreinforced and reinforced masonry prisms and address the potential benefits of using the proposed embedded boundary elements in the wall design and discuss the shortage of the current Canadian codes [6, 7].

BEHAVIOUR OF MASONRY PRISMS SUBJECTED TO MONOTONIC COMPRESSION

The use of concrete hollow blocks with the thickness over 250 mm is rare in Canada, but deeper blocks are needed for the TRM buildings because they reduce the axial stress level and more vertical reinforcement can be accommodated in the cores inside the cores. With four vertical reinforcing bars supporting the four corners of closely spaced rectangular ties in the confined grouting cores at the wall ends, where are the critical regions that damage might be concentrated, increasing wall ductility, rotation capacity and even moment capacity. Therefore, the focus of the first phase of the project is to examine the mechanical properties of masonry prisms using 250 mm hollow concrete blocks with different reinforcement detailing. Larger core space in 250 mm blocks can be easily placed with four 20M vertical rebars inside each core, but the middle web of the blocks had to be removed for configurations of horizontal ties are shown in Figure 1. and were designed to confine the grout core and restrain the vertical reinforcement from buckling. RM prisms with different tie spacings (100 mm and 200 mm) will also be tested respectively. The test matrix consisted of fifty-three 4-course prism specimens. Out of these, five specimens were unreinforced hollow prisms, and eight were unreinforced but grouted prisms, while the remaining specimens had different reinforcement arrangements. The compressive strength of single concrete block units averaged 20.5 MPa, while the compressive strength of three 28-day grout cylinders averaged 26.5 MPa, and the compressive strength of three 28-day mortar cubes averaged 22.6 MPa. The expected outcomes of this phase are not only to determine the masonry compressive strength (f'_m), but also measure and quantify the stress-strain behaviour of the unreinforced and reinforced prisms under different tie detailing.

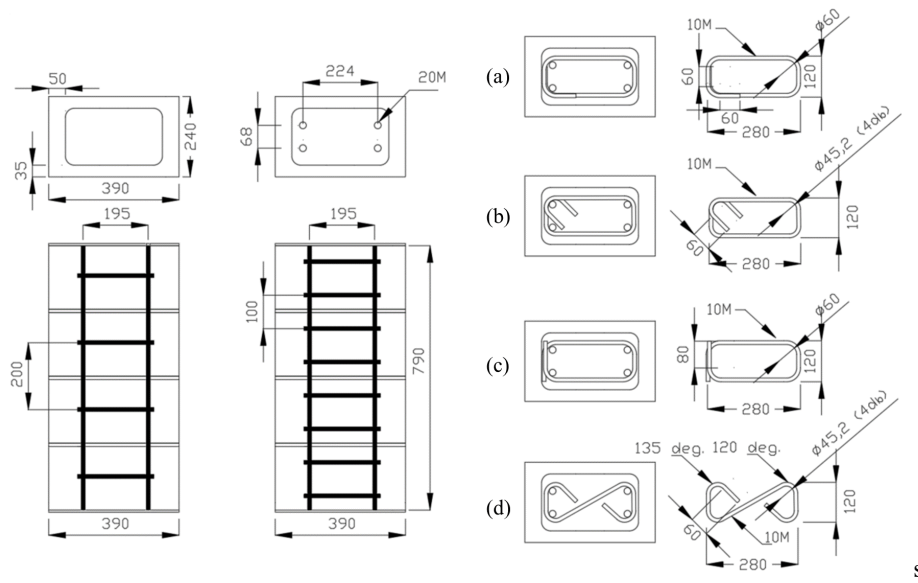


Figure 1. Reinforced masonry (RM) prism specimens: (a) 90-degree hooks, (b) 135-degree hooks, (c) over-lapping ties, and (d) S-shaped configuration.

Instrumentation and test setup

For the purpose of testing the RM prism specimens, a lever-arm test setup is proposed and shown in Figure 2. The lever-arm testing system was designed to amplify the compression force of the hydraulic actuator in order to test higher compressive capacity of RM prisms. The setup includes a deep strong horizontal loading beam and a vertical column connected with a pin joint. The beam and the column are stacked by several steel H-beam units with welded stiffeners and end plates which can be connected by high strength bolts to create different configuration to satisfy the experimental requirements and different sizes of specimens. A hydraulic actuator with a force capacity of 2000 kN (450 kips) is mounted on the free end of the loading beam to induce compression in the RM prism specimen at the middle of the loading beam.

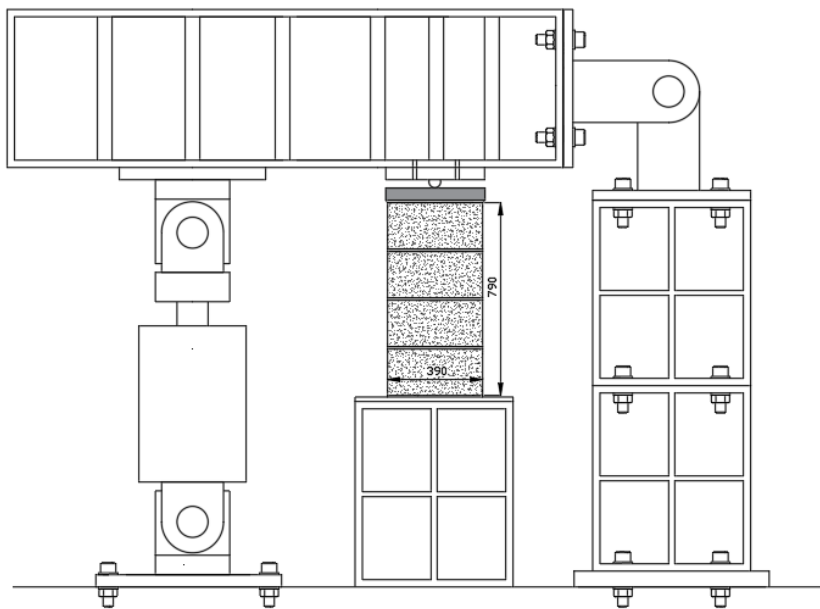


Figure 2. Proposed test setup for RM prisms under uniaxial compression.

The displacement measurement is critical to obtain the stress-strain behaviour of RM prisms. In this project, two methods are used to measure the displacement. The first method measures the deformation of the prisms by two linear potentiometers installed on the aluminum brackets as shown in Figure 3(a). The two brackets are screwed, and the screws slightly touch the surfaces of the prism and hold the brackets with friction. Two potentiometers are mounted on the front and back side of the

top brackets, and their strokes are extended by tensioned strings hooked on the bottom bracket. The gauge length is the distance between the two brackets which is 615 mm. The second measurement uses contactless vision-based tracking technology. The deformation of the prisms was measured by tracking high contrast patterns shown in Figure 3(b) which were stuck on the specimen surface by epoxy. High-resolution photos were taken every two seconds during the whole test and the Kanade-Lucas-Tomasi (KLT) feature tracker algorithm was implemented to analyze the movement of the patterns from the photo sets.

A four-coursed hollow prism was tested as a dummy specimen to check the capability of the testing facility and the vision-based displacement measurement. The maximum compressive strength of the four-course hollow prism was 19.2 MPa (based on the maximum force of 851 kN and the net area of 44300 mm²). Followed by the hollow prism, two four-course unreinforced grouted prisms were tested, and both remained elastic when the testing facility reached the maximum force capacity of 1788 kN (400 kips). The equivalent compressive strength for the two grouted prisms was 19.1 MPa, considering the gross cross-section dimensions of 390 mm by 240 mm. The two specimens showed that, without the middle web, the grouted core might contribute more to the overall prism strength compared to the two grouted cores divided by the middle web of the complete two-cell blocks, which potentially causes larger f'_m , and even greater than the block compressive strength, f_{bl} . The behaviour of prisms with middle web removed was not in line with the experimental observations from the previous grouted masonry prism studies [16] In order to directly identify the stress-strain property of the grouting core inside the RM prisms, the block shells and the exterior webs of grouted prisms were removed by the wheel saw with diamond blade. One of the two prisms was unreinforced and the other was reinforced by four 20M vertical rebars and 10M ties with 135-degree hooks placed at 100 mm spacing as shown in Figure 3(c). The dimensions of the unreinforced and reinforced grout cores were 170 mm by 285 mm. The tested reinforced grouted core was shown on Figure 3(d). The deformation determined by distance change between the patterns on the top and the base of the core was used to calculate the average strain of the core. The results were plotted on Figure 4. with the stress-strain curves of grout cylinders measured using the same vision-based method. Although two specimens are not sufficient considering the variability in the grout strength and concrete block strength, the results showed the effectiveness of the reinforcement for confining the grouted core and potentially increasing the grout strength and the ultimate compressive strain. The maximum compressive strength of unreinforced and reinforced grout core were 20 MPa and 30 MPa respectively.

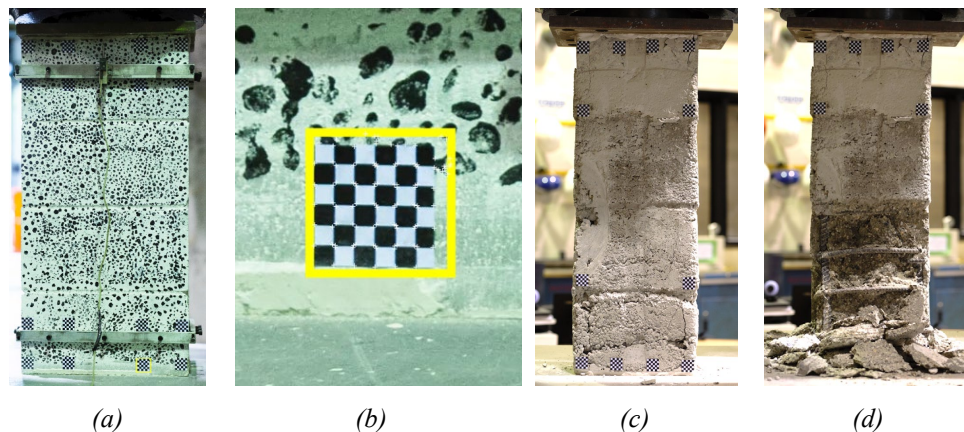


Figure 3 Testing of RM prisms: (a) prism specimens with brackets and potentiometers; (b) patterns tracked by KLT algorithm; (c) reinforced grouting core specimen; and (d) tested reinforced grouting core specimen.

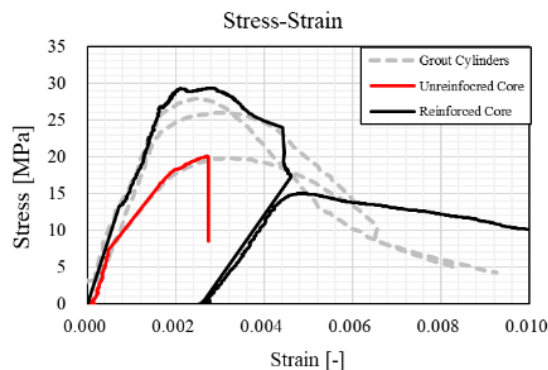


Figure 4. Preliminary experimental result.

Several researchers proposed empirical prediction equations to determine the f'_m value based on design parameters, such as block strength, grout strength and mortar strength. The weights of the grout strength contribution on those studies varies from 0.23 to 0.94 A_{core}/A_g [17-21]. The preliminary results, although not representative due to the small number of samples, indicate that the equivalent masonry compressive strength could be determined through the following Eq. (1):

$$f'_{m,eqv} = (f_{bl}A_{net} + f_{gr}A_{core})/A_g \quad (1)$$

where f_{bl} is the compressive strength of the concrete block unit; A_{net} is the net cross-sectional area of the block with removed middle web; f_{gr} is the cylinder compressive strength of the grout; A_{core} is the cross-sectional area of the grout core; A_g is the gross cross-sectional area of the grouted prism. In the case of the 250 mm blocks used in this study, the maximum masonry compressive strength can be calculated as Eq. (2), where the contribution weight of the grout is surprisingly high compared to the previous studies.

$$f'_m = 0.47f_{bl} + 0.53f_{gr} \quad (2)$$

COMPONENT-LEVEL TESTING: RM SHEAR WALLS UNDER COMBINED AXIAL LOAD & FLEXURE

The boundary zones are the main contributor of the resultant compressive force at the wall base to form the moment capacity, and those zones will have concentrated damage due to the large tensile and compressive strain. The advantage of confined boundary elements is to mitigate the concrete spalling and bar-buckling; therefore, preventing toe-crushing and rocking failure mechanisms from activation at small storey drift. The confined embedded boundary elements, which are the focus of the ongoing research project can increase the moment capacity of the RMSWs. Moreover, the stress-strain behaviour of the RM prisms shows increased peak strength and larger ultimate strain due to the confinement effect. The design of embedded boundary elements that will be used to enhance the performance of the RMSWs can be performed using Eq. (3) which estimates the moment capacity (M_r) of rectangular RMSWs with concentrated reinforcement at the wall ends and distributed reinforcement along the wall length [22]. (See Figure. 5)

$$M_r = C_m \left(\frac{t_w - a}{2} \right) + 2(\phi_s f_y A_{BE}) \left(\frac{t_w}{2} - d' \right) \quad (3)$$

$$, \text{ where } C_m = P_f + \phi_s f_y A_d$$

where C_m is the equivalent compressive force; a is compression zone depth which can be determined from Equation (3); A_{BE} is the total area of the concentrated vertical reinforcement at the ends; d' is the distance from the extreme compression fibre to the centroid of the concentrated compression reinforcement; f_y is the steel yield strength; P_f is applied axial force acting on the wall; and A_d is the total area of the distributed vertical reinforcement along the wall length.

The wall compression zone depth calculated from Eq. (4) as follows.

$$a = \frac{(P_f + \phi_s f_y A_d)}{0.85 \phi_m f'_m t_w} \quad (4)$$

The compression zone would be likely contained within the confined boundary regions due to the higher masonry compressive strength that observed in the first phase. It is important to use the correct value of the masonry compressive strength in the moment capacity design. It is straightforward that vertical reinforcement is placed within the end wall cells and that higher masonry strength be used in order to achieve higher wall moment capacity. However, from the perspective of the code-based ductility requirements of the RMSWs, high amount of the vertical reinforcement and high axial stress on the wall are typically not allowed due to the c/l_w limitation shown in Eq. (5).

$$\frac{c}{l_w} = \frac{a}{\beta_1 l_w} \leq \frac{\epsilon_{mu}}{0.01} \text{ (Moderately DRMSWs)} \quad (5a)$$

$$\frac{c}{l_w} = \frac{a}{\beta_1 l_w} \leq \frac{\epsilon_{mu}}{0.012} \text{ (DRMSWs)} \quad (5b)$$

where c is the neutral axis depth; β_1 is taken as 0.8 for f'_m less than 20 MPa; ϵ_{mu} is the masonry compressive strain limit.

If amount of vertical reinforcement in the wall is excessive or applied axial stress is too high, the concrete in the compression zone will crush before the reinforcement yields, resulting in brittle compression-controlled flexure failure. Considering the masonry compressive strain limit (ϵ_{mu}) of 0.0025 in the Eq. (4), CSA S304-14 implicitly sets the maximum c/l_w ratio of 0.208 and 0.25 for the ductile RMSWs and moderately ductile RMSWs respectively to avoid the brittle damage and

guarantee the rotational capacity of the RMSWs. Nonetheless, regarding the design of TRM buildings, a higher amount of gravity load should be considered. The existing code provisions and the DRMSW category still make the design difficult. For instance, if the ϵ_{mu} is taken greater than 0.0025 is required to perform the experimental testing and analysis to specify the level of strain and demonstrate the ductility capacity of the wall is required by the code. Therefore, a new type of RMSWs with the embedded boundary elements that will have enhanced seismic performance and extra benefits from higher masonry compressive strength and more ductile masonry properties due to the confined grout core is designed and will be tested in this phase.

The prototype of RMSW with embedded boundary elements is shown in Figure 6(a). Four 20M bars and 10M horizontal ties will be installed into the blocks with removed middle-web at the exterior two cells at both ends of the wall. Due to the running bonds, the embedded boundary elements will be formed by two patterns alternatively every other course. One pattern uses a middle-web-removed double ender block, noted as the “O” block, and the other pattern is formed by one half-block with single end shell removed, (“C” blocks), plus one stretcher block with single exterior web removed, (“A” blocks). With the “O” and “C plus A” block patterns, vertical reinforcement and horizontal ties can be easily installed into the boundary blocks. As the control group, ductile RMSWs shown in Figure 6(b) were designed and detailed following the CSA S304-14 code requirements and will be tested as well. In addition, the seismic performance of partially grouted RMSWs in Figure 6(c) will be also tested in this phase. All wall specimens were designed with 3.8 m height, 2.6 m length using 250 mm masonry units. These three types of RMSW specimens were proposed to fill a research gap regarding the experimental evidence for future applications. [23]

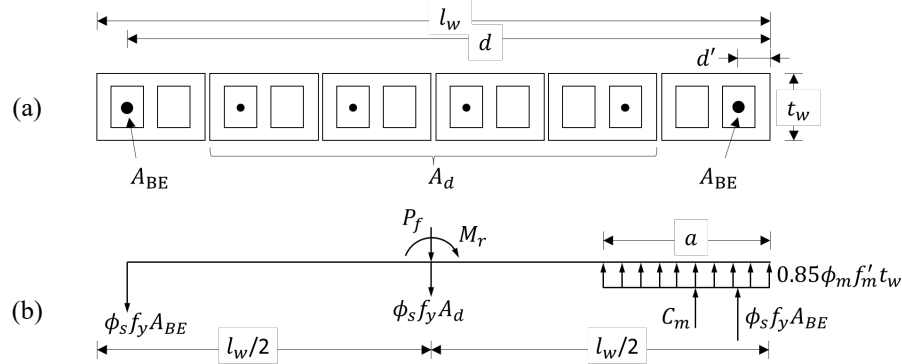


Figure 5. Simplified design model for rectangular wall section: (a) plan view cross-section showing reinforcement; (b) internal force distribution.

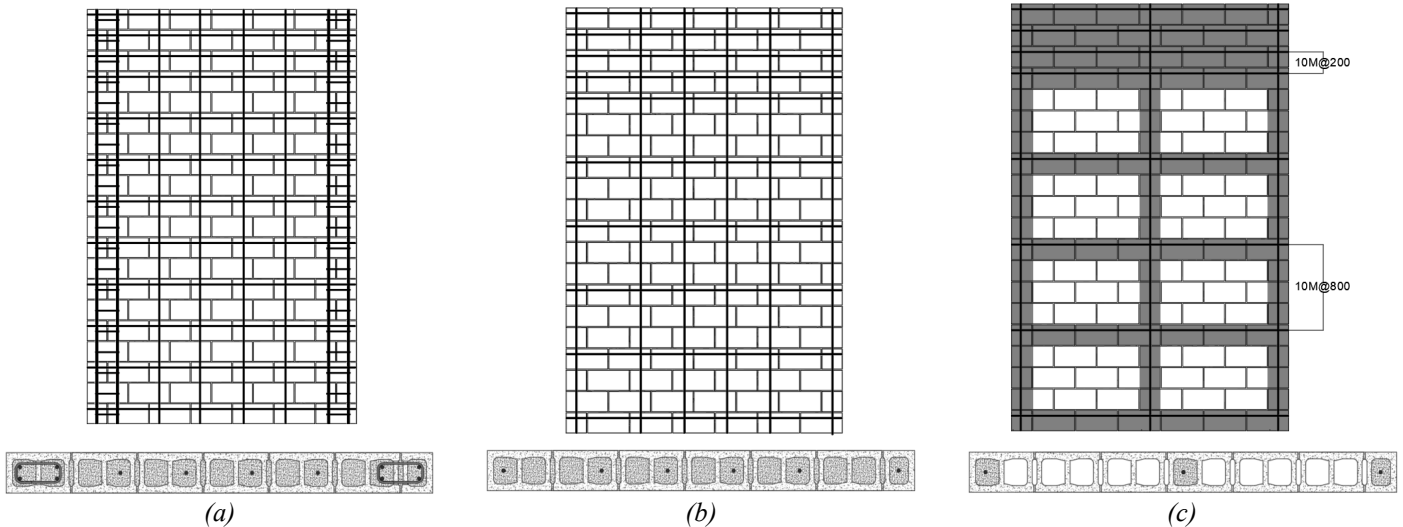


Figure 6. RMSW specimens: (a) DRMSW with embedded boundary elements, (b) fully grouted DRMSW, and (c) partially grouted RMSWs.

Test setup

Figure 7 shows a two-dimensional test setup for the wall testing, which is capable of controlling the three degree-of-freedom (DOFs) at the top of the wall through a three-hydraulic-actuator configuration. The wall specimen is placed between two steel channels at the top. Additional dowels are required to strengthen the top of the wall to successfully transfer the horizontal shear, axial force, and overturning moment to the RC footing, which is mounted to the strong floor with PT bars to resist the lateral movement and rotation at the wall base. The two steel channels are bolted on two extension pieces of steel loading beams. The beams are formed by modular steel H-beam units with the stiffeners. Each extension loading beam is connected to a vertical hydraulic actuator, which is mounted on the strong floor. One of the loading beams is also connected to a horizontal hydraulic actuator mounted on the reaction wall. The two vertical actuators will apply a permanent axial force on the wall and be programmed to adjust their forces to simultaneously apply an additional overturning moment on the wall according to the lateral force provided by the horizontal actuator. The horizontal actuator will be displacement-controlled to push and pull the loading beam following a cyclic loading protocol.

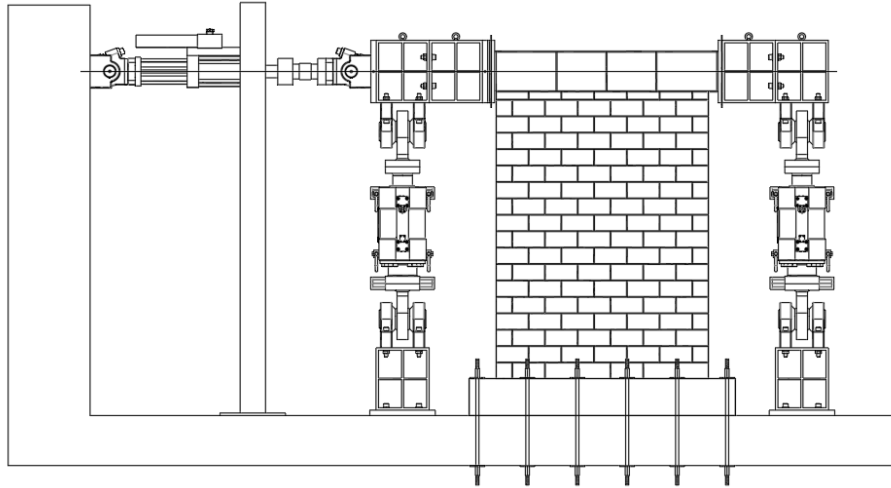


Figure 7. Proposed 3-DOF test setup for the cyclic quasi-static testing on RMSWs.

SYSTEM-LEVEL TESTING: HYBRID SIMULATION

Limited RM system specimens have been tested before. Several 1/3rd scale specimens of 2-story prototype RM buildings were subjected to reversed quasi-static loading to observe the effect of asymmetric building layout, the wall-to-slab interaction, effect of coupled walls and flanged walls, and the influence of the diaphragm rigidity [24-26]. The dynamic systematic behaviour of RM buildings was observed through testing of 2- and 3-story full-scale fully grouted and partially grouted RM building specimens on a shaking table [27-29]. Although shake table tests and quasi-static tests of RM building specimen provided valuable experimental data on seismic behaviour of RM buildings, it would be expensive and challenging to conduct similar experiments on TRM building specimens with higher aspect ratio and higher axial stress level would be expensive and challenging due to the limited capacity of the current experimental facilities.

Hybrid simulation testing could be a promising solution for addressing this issue. Given that ductile RMSWs in TRM buildings are intended to show flexure-dominant behaviour, it is expected that the plastic hinge region, where the nonlinear deformation and damage concentrated, is situated at the lower portion of tall RMSWs. By solely testing the base of slender RMSWs and employing numerical models to simulate the remaining portion, it is feasible to assess the overall performance of TRM buildings at the system level. A hybrid experimental and numerical simulation will be performed at the system level to obtain the seismic response of a TRM building subjected to earthquake excitation.

Hybrid simulation framework and control algorithms

The proposed hybrid simulation framework is shown in Figure 8. The 2D 3-DOF test setup for RMSWs will be further integrated with the ACTS controller. The controller has two physical devices, namely industrial programmable controller (IPC) and data acquisition system (DAS) combined with signal processing modules (SPMs). IPC is basically a computer that can run software and programming scripts to process the signals and conduct analysis of numerical models, while the DAS and SPMs serve as I/O channels that can receive input signals from the external sensors and send output signals to control the servo-valves of the hydraulic actuators. The two devices are connected to communicate and form the control loop. The hardware can be operated by advanced low-level controller (ALC) and hardware-in-the-loop hybrid simulation software

(HSS). ALC is a graphical user interface that directly shows all the signal values and does the real time signal editing, such as filters and controlling algorithms. ALC is a bridge between hardware, i.e., hydraulic systems, and the numerical analysis platform, HSS, to achieve hybrid simulation testing. HSS is numerical modeling software that can be embedded with any user-defined nonlinear material models, element models, and nonlinear integration algorithms. Experimental elements that consider the geometric transformation between physical substructures and numerical substructures are developed to update the stiffness matrix and structural response (i.e., nodal forces, and nodal displacements) from the experimental setup and then send the next-step iterated simulated numerical results to the controllers as command signals to drive the hydraulic system. The mixed-control algorithms based on the switch-control algorithm developed by Yang et al. [30] will be implemented to control the three actuators in synchronization. Yang et al. [30] developed a reliable displacement-based control algorithm and force-based control algorithm and were able to test specimens with varying stiffness by switching between the two algorithms to ensure the accuracy. In the case of 3-DOF controlling system in this project, two vertical actuators will be controlled by force-based algorithms to provide a permanent compressive force simulating the gravity load and an overturning moment at the top of the tested RMSW simulating the inter-storey moment, while the horizontal actuator will be controlled by displacement-based algorithms.

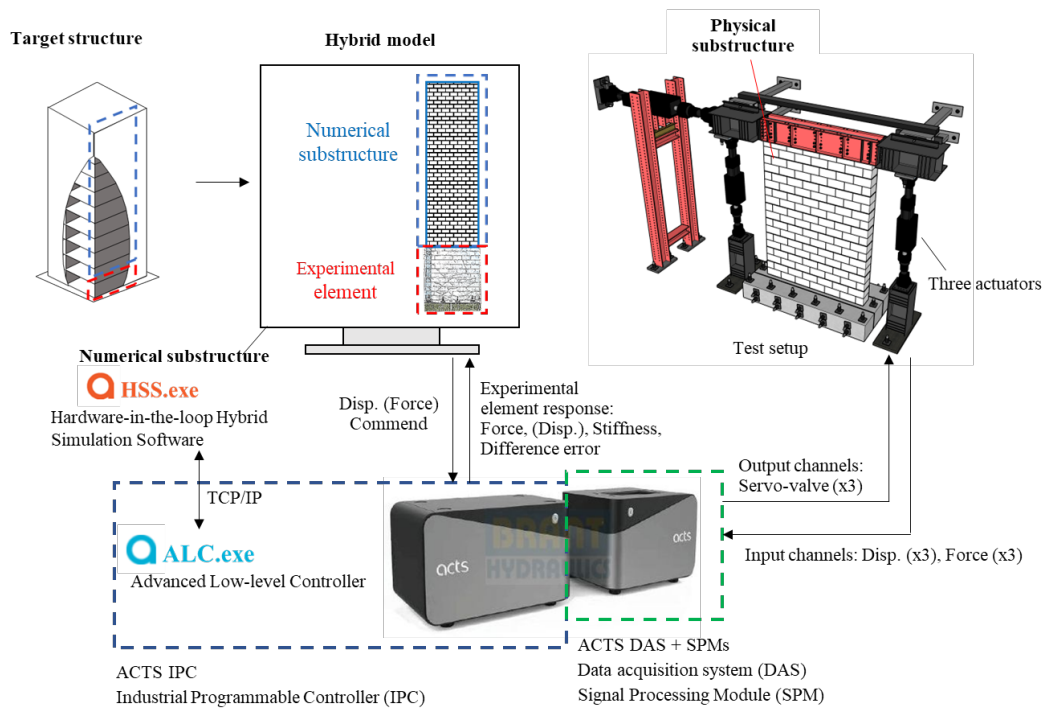


Figure 8. Proposed hybrid simulation testing framework.

CONCLUSIONS

An initial stage of an experimental research project focused on investigating the seismic response of TRM shear walls for masonry field applications in Canada is in progress at the UBC Department of Civil Engineering. This comprehensive research program comprises both robust experimental and analytical components. The specimens, featuring RM walls with high aspect ratios suitable for medium-rise to tall buildings, are designed to exhibit flexure-dominant behavior. The research will examine the seismic response of TRM shear walls at three distinct levels: material/assembly, component, and system.

Hybrid simulation testing represents a promising approach for understanding the seismic response of TRM buildings, as it is not constrained by the capacity of experimental facilities. Prior to conducting hybrid testing, however, it is necessary to study the behavior of individual walls in order to develop a reliable numerical model for RM building.

ACKNOWLEDGMENTS

The authors would like to acknowledge the support from NSERC Alliance Grant, and industry partners Canada Masonry Design Centre (CMD), Canadian Concrete Masonry Producers Association (CCMPA), and Harris Rebar (Nucor®).

REFERENCES.

- [1] Drysdale, R. G., and Hamid, A. (2005). *Masonry structures: behavior and design*. Mississauga, ON: Canada Masonry Design Centre.
- [2] Hamid, A. (2018). *Masonry Structures: Behaviour and Design*. Fourth Edition, The Masonry Society, USA.
- [3] Corrêa, M.R.S. (2012). Masonry Engineering in Brazil: Past Development, Current Overview, Future Improvements. *Proc., 15th Int. Brick and Block Masonry Conf.*, Florianópolis, Brazil.
- [4] Wang, F. L., Zhang, X. C., and Zhu, F. (2016). Research progress and low-carbon property of reinforced concrete block masonry structures in China. *Proc., 16th Int. Brick and Block Masonry Conf.*, Padova, Italy.
- [5] El-Dakhkhni, W., and Ashour, A. (2017). Seismic response of reinforced concrete masonry shear-wall components and systems: State of the art. *J. Struct. Eng.* 143 (9): 03117001. [https://doi.org/10.1061/\(ASCE\)ST.1943-541X.0001840](https://doi.org/10.1061/(ASCE)ST.1943-541X.0001840).
- [6] NRC (2020). National Building Code of Canada 2020, *National Research Council*, Ottawa, ON, Canada. <https://doi.org/10.4224/W324-HV93>.
- [7] Canadian Standard Association - CSA (2014). *CSA S304: Design of masonry structures*. Prepared by the CSA, Mississauga, Ontario, Canada.
- [8] Pantazopoulou, S. J. (1998). "Detailing for Reinforcement Stability in RC Members." *J. Struct. Eng.*, 124 (6): 623–632. [https://doi.org/10.1061/\(ASCE\)0733-9445\(1998\)124:6\(623\)](https://doi.org/10.1061/(ASCE)0733-9445(1998)124:6(623)).
- [9] Moyer, M. J., and Kowalsky, M. J. (2003). "Influence of Tension Strain on Buckling of Reinforcement in Concrete Columns." *SJ*, 100 (1): 75–85. <https://doi.org/10.14359/12441>.
- [10] Berry, M., and M. Eberhard. (2005). "Practical Performance Model for Bar Buckling." *Journal of Structural Engineering-asce - J STRUCT ENG-ASCE*, 131. [https://doi.org/10.1061/\(ASCE\)0733-9445\(2005\)131:7\(1060\)](https://doi.org/10.1061/(ASCE)0733-9445(2005)131:7(1060)).
- [11] ACI Committee 318. (2019). Building Code Requirements for Structural Concrete (ACI 318-19) and Commentary (318R-19). Farmington Hills, Michigan: American Concrete Institute.
- [12] Canadian Standard Association - CSA (2014). *CAN/CSA-A23.3: Design of concrete structures*. Prepared by the CSA, Mississauga, Ontario, Canada.
- [13] Shedid, M. T., El-Dakhkhni, W. W. and Drysdale R. G. (2010). "Characteristics of Rectangular, Flanged, and End-Confined Reinforced Concrete Masonry Shear Walls for Seismic Design." *J. Struct. Eng.*, 136 (12): 1471–1482. [https://doi.org/10.1061/\(ASCE\)ST.1943-541X.0000253](https://doi.org/10.1061/(ASCE)ST.1943-541X.0000253).
- [14] Banting, B. R., and W. W. El-Dakhkhni. (2014). "Seismic Design Parameters for Special Masonry Structural Walls Detailed with Confined Boundary Elements." *J. Struct. Eng.*, 140 (10): 04014067. [https://doi.org/10.1061/\(ASCE\)ST.1943-541X.0000980](https://doi.org/10.1061/(ASCE)ST.1943-541X.0000980).
- [15] Aly, N., and K. Galal. 2020. "In-plane cyclic response of high-rise reinforced concrete masonry structural walls with boundary elements." *Engineering Structures*, 219: 110771. <https://doi.org/10.1016/j.engstruct.2020.110771>.
- [16] Sarhat, S. R., and E. G. Sherwood. (2018). "Compressive Strength Prediction of Grouted Hollow Concrete Block Masonry: A Comparative Study of Major International Codes and a Proposed Model." *TMS Journal*, 36: 1–33.
- [17] Hamid, A. A., Drysdale, R. G., and Heidebrecht, A. C. (1978). "Effect of Grouting on the Strength Characteristics of Concrete Block Masonry." *Proceedings of the North American Masonry Conference*, Boulder, CO.
- [18] Sarhat, S. R. (2016). "The Size Effect and Strain Effect in Reinforced Masonry." Carleton University.
- [19] Mohamed, M. Y. M. 2018. "Compressive Stress-strain of Unreinforced Masonry Boundary Element Prisms." masters. Concordia University.
- [20] Sturgeon, G. R., Longworth, J., and Warwaruk, J. (1980). *An Investigation of Reinforced Concrete Block Masonry Columns*. University of Alberta Structural Engineering Report No. 91, Edmonton, AB, Canada.
- [21] Priestley, M. J. N., and Chai Yuk Hon. (1984). "Prediction of Masonry Compression Strength Part:1." *New Zealand Concrete Construction*, 28, 11–14.
- [22] Brzev, S. and Anderson, D.L. (2018). *Seismic Design Guide for Masonry Buildings*. Second Edition, Canadian Concrete Masonry Producers Association, Toronto, Ontario, Canada (www.ccmpa.ca).
- [23] Hsu, Y.-C., M. Dou, T. Y. Yang, and S. Brzev. (2022). "ULTIMATE DRIFT CAPACITY OF FLEXURE-DOMINANT REINFORCED CONCRETE MASONRY SHEAR WALL." *CSCC 2022 Annual Conference*. Whistler, Canada.
- [24] Heerema, P., M. Shedid, D. Konstantinidis, and W. El-Dakhkhni. (2015). "System-Level Seismic Performance Assessment of an Asymmetrical Reinforced Concrete Block Shear Wall Building." *Journal of Structural Engineering*, 141 (12): 04015047. American Society of Civil Engineers. [https://doi.org/10.1061/\(ASCE\)ST.1943-541X.0001298](https://doi.org/10.1061/(ASCE)ST.1943-541X.0001298).
- [25] Ashour, A., W. El-Dakhkhni, and M. Shedid. (2016). "Experimental Evaluation of the System-Level Seismic Performance and Robustness of an Asymmetrical Reinforced Concrete Block Building." *Journal of Structural Engineering*, 142 (10): 04016072. American Society of Civil Engineers. [https://doi.org/10.1061/\(ASCE\)ST.1943-541X.0001529](https://doi.org/10.1061/(ASCE)ST.1943-541X.0001529).
- [26] Ezzeldin, M., L. Wiebe, and W. El-Dakhkhni. (2017). "System-Level Seismic Risk Assessment Methodology: Application to Reinforced Masonry Buildings with Boundary Elements." *J. Struct. Eng.*, 143 (9): 04017084. [https://doi.org/10.1061/\(ASCE\)ST.1943-541X.0001815](https://doi.org/10.1061/(ASCE)ST.1943-541X.0001815).

- [27] Mavros, M., F. Ahmadi, P. B. Shing, R. E. Klingner, D. McLean, and A. Stavridis. (2016). “Shake-Table Tests of a Full-Scale Two-Story Shear-Dominated Reinforced Masonry Wall Structure.” *Journal of Structural Engineering*, 142 (10): 04016078. American Society of Civil Engineers. [https://doi.org/10.1061/\(ASCE\)ST.1943-541X.0001528](https://doi.org/10.1061/(ASCE)ST.1943-541X.0001528).
- [28] Stavridis, A., F. Ahmadi, M. Mavros, P. B. Shing, R. E. Klingner, and D. McLean. (2016). “Shake-Table Tests of a Full-Scale Three-Story Reinforced Masonry Shear Wall Structure.” *Journal of Structural Engineering*, 142 (10): 04016074. American Society of Civil Engineers. [https://doi.org/10.1061/\(ASCE\)ST.1943-541X.0001527](https://doi.org/10.1061/(ASCE)ST.1943-541X.0001527).
- [29] Koutras, A. A., and P. B. Shing. (2020). “Seismic behavior of a partially grouted reinforced masonry structure: Shake-table testing and numerical analyses.” *Earthquake Engineering & Structural Dynamics*, 49 (11): 1115–1136. <https://doi.org/10.1002/eqe.3281>.
- [30] Yang, T. Y., D. P. Tung, Y. Li, J. Y. Lin, K. Li, and W. Guo. (2017). “Theory and implementation of switch-based hybrid simulation technology for earthquake engineering applications: Switch-based hybrid simulation for earthquake engineering.” *Earthquake Engng Struct. Dyn.*, 46 (14): 2603–2617. <https://doi.org/10.1002/eqe.2920>.